Argonne NATIONAL LABORATORY

... for a brighter future

Investigations of coupled biogeochemical processes affecting the transformation of U: Integration of synchrotron-based approaches

Ken Kemner and Ed O'Loughlin

Environmental Remediation Science Program PI Meeting

April 19, 2007

U.S. Department of Energy

UChicago Argonne LLC

Office of Science U.S. DEPARTMENT OF ENERGY

*It is necessary to **directly** determine the speciation of elements in hydrobiogeochemical systems. It is **not wise** to **assume** or **indirectly** determine the speciation of an element.*

Scientifically integrated lab-based and synchrotron approaches directly provide this information and enable an iterative process of science driving the development of new synchrotron-based technology and the technology providing important insights that allow development of new scientific hypotheses.

ERSP-supported access to synchrotrons

- Advanced Photon Source: Bruce Ravel, Shelly Kelly, Ken Kemner
- Advanced Light Source: Peter Nico, Susan Hubbard
- National Synchrotron Light Source: Jeff Fitts, Paul Northrup
- Stanford Synchrotron Radiation Laboratory: Sam Webb, John Bargar

Acknowledgements

- ANL-Biosciences Division (Molecular Environmental Science Group)
  - E. O'Loughlin (Biogeochemist)
  - M. Boyanov, S. Kelly, B. Ravel (X-ray Physicists/Spectroscopists)
  - D. Sholto-Douglas, K. Skinner-Nemec (Microbiologists)
- ANL-Advanced Photon Source
  - B. Lai, J. Maser, Z. Cai (X-ray Microscopist)
- Pacific Northwest National Laboratory
  - J. Fredrickson, M. Marshall,A. Beliaev (Geo-, Molecular- Microbiologists)
  - A. Dohnalkova, J. Kennedy, J. Zachara (Electron Microscopist, Geochemist)
- Uniformed Services University of the Health Sciences
  - M. Daly (Microbiologist)
- Oak Ridge National Laboratory
  - S. Brooks, P. Jardine, D. Watson (Soil/Geo Chemists)
- Stanford University
  - C. Criddle, W. Wu (Env. Engineering and Microbiology)
- U. of Southern California
  - K. Nealson (Microbiologist, Geomicrobiologist)

Synchrotrons- “X-ray Physics 101”

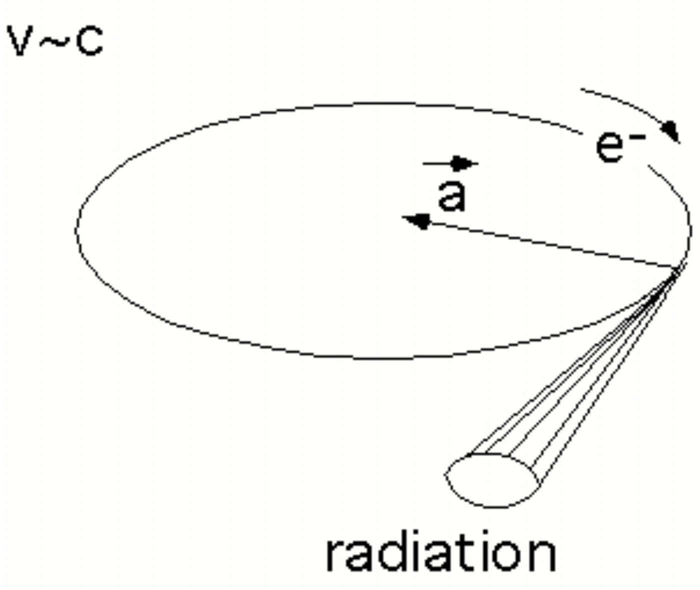

The Advanced Photon Source, Argonne National laboratory

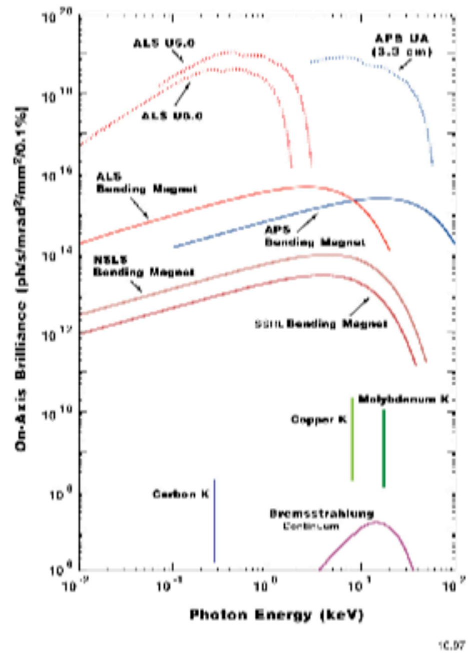

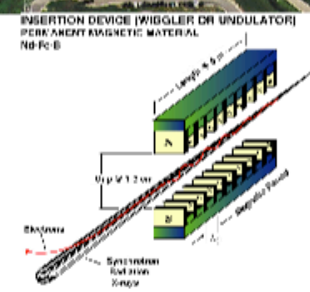

MRCAT/ENVIROCAT is a dedicated hard x-ray insertion device beam line dedicated to x-ray absorption (micro)spectroscopy and limited x-ray fluorescence imaging. Development of a bending magnet beam line for increased spectroscopy availability and development of improved x-ray fluorescence imaging capabilities at the insertion device beam line are presently underway.

X-ray-Absorption Fine Structure (XAFS)

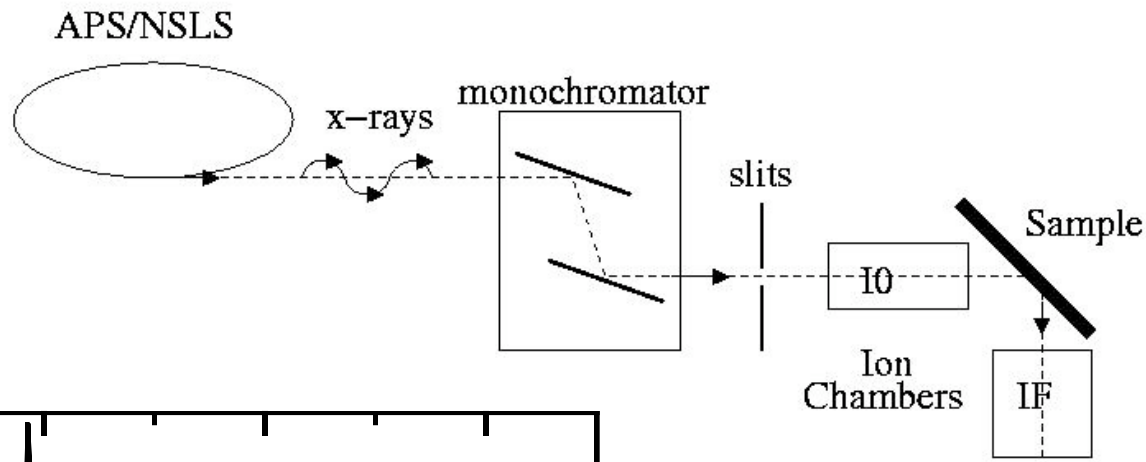

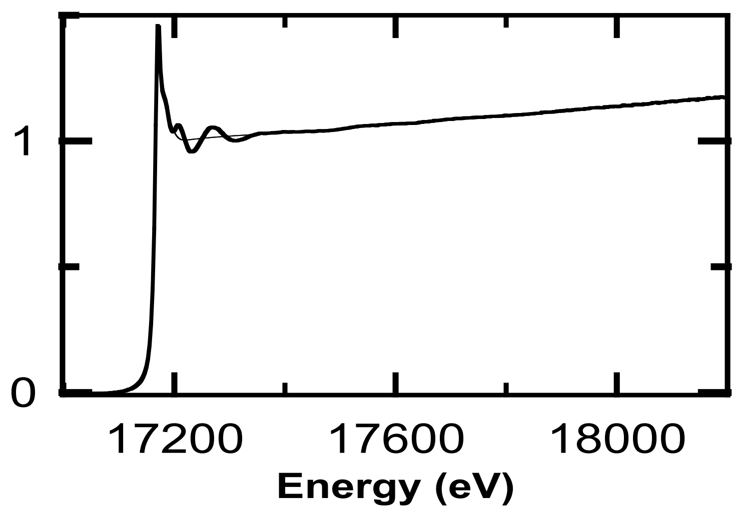

- Attenuation of x-rays

  $I_t = I_0 e^{-\mu(E) \cdot x}$

- Absorption coefficient

  $\mu(E) \propto I_f / I_0$

X-ray Absorption Near Edge Structure-(XANES)

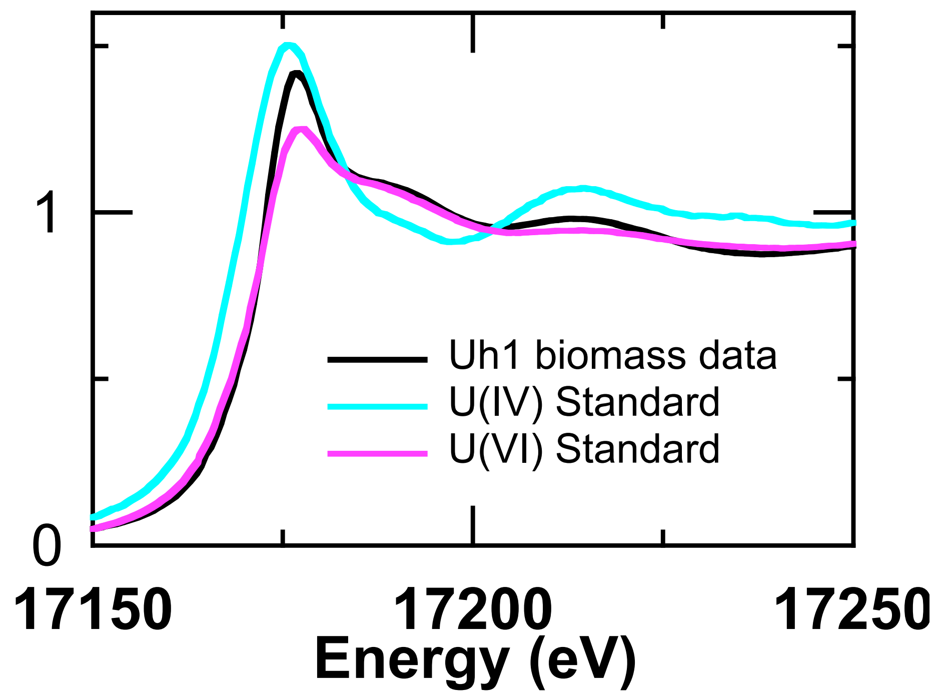

- Position of edge depends on valence state of absorbing atoms

Extended X-ray Absorption Fine Structure- (EXAFS)

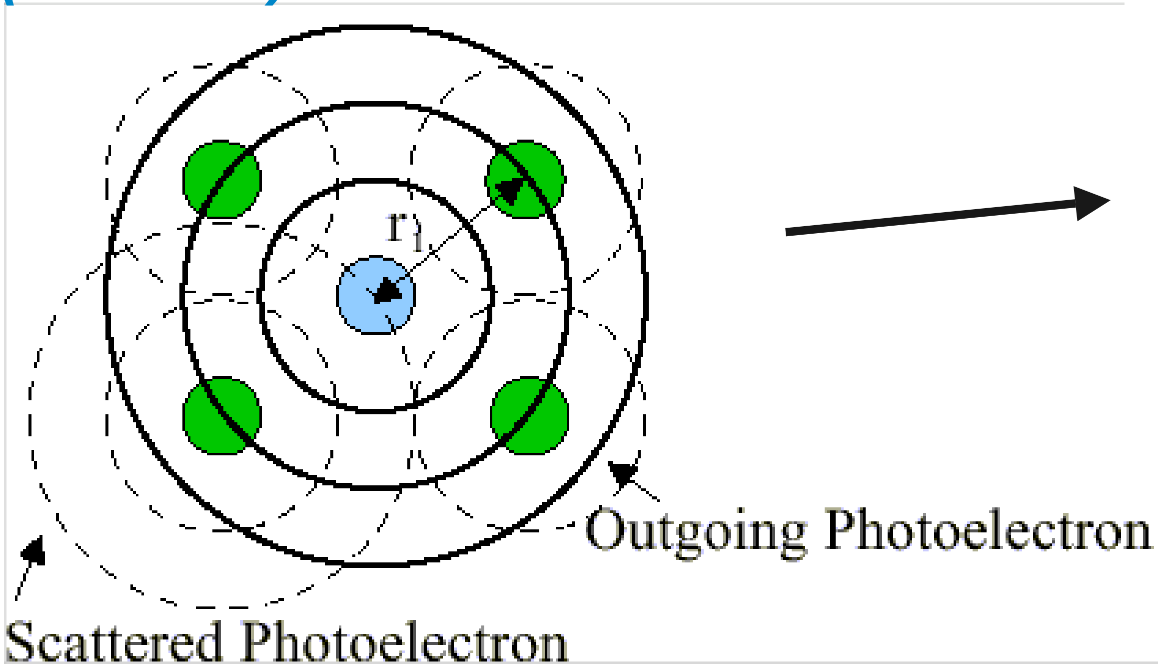

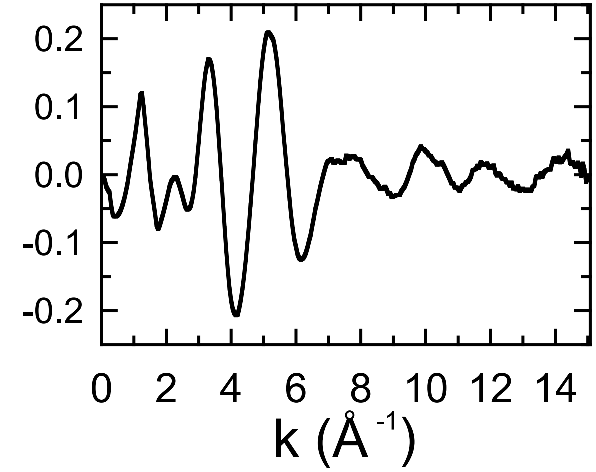

Fourier Analysis

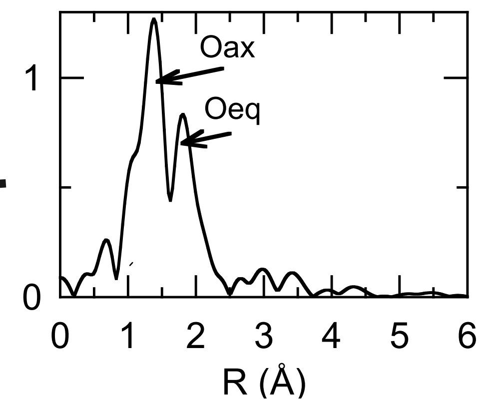

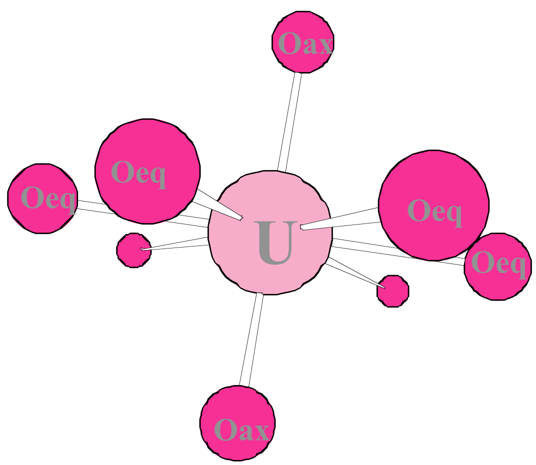

- **Like an atomic radial distribution function**
  - Distance
  - Number
  - Type
  - Structural disorder

Electron transfer from Fe to U at carboxyl surfaces

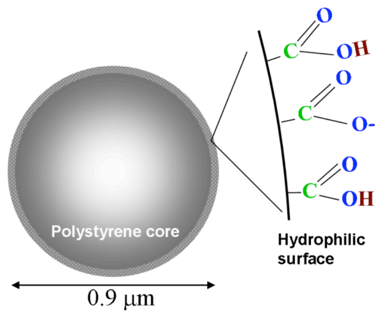

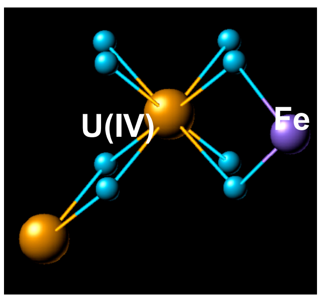

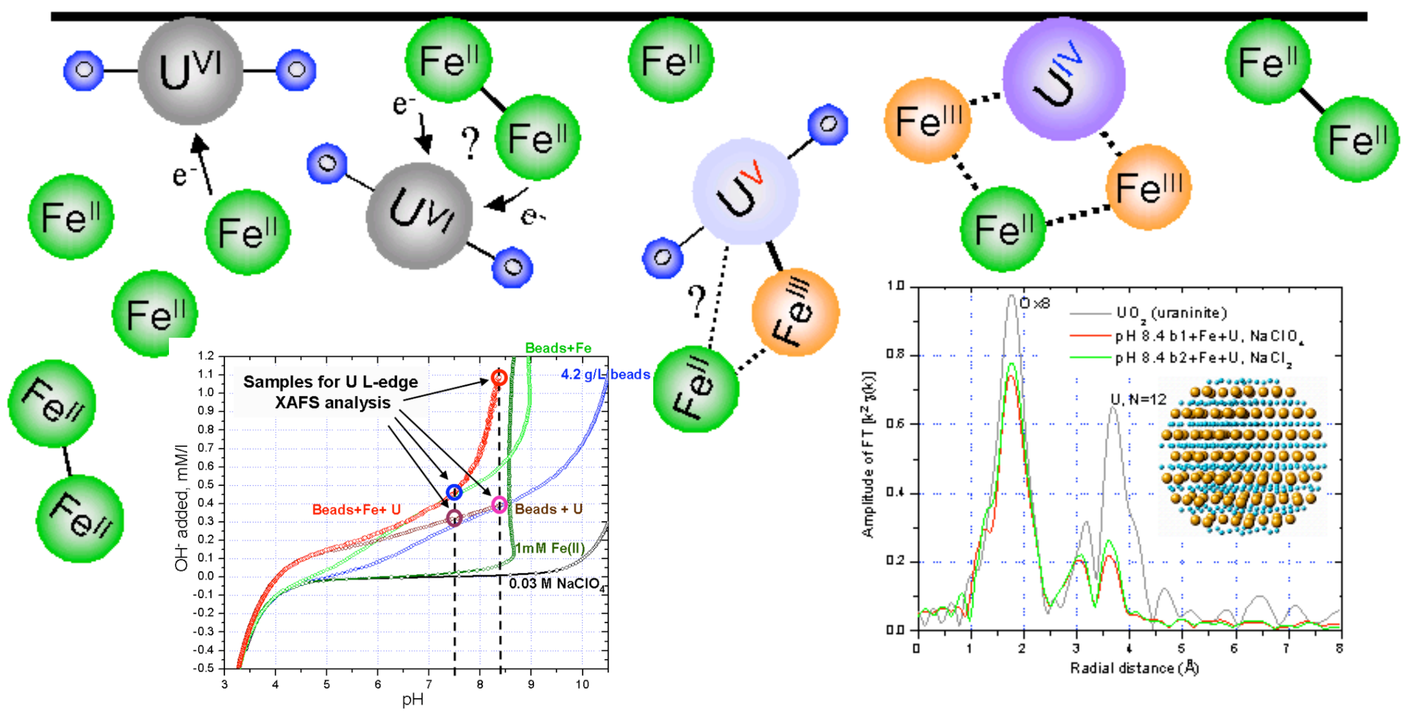

Adsorbed or solvated monomeric Fe(II) does not reduce U(VI) (pH 7.5)

Rapid reduction of adsorbed U(VI) to U(IV) is observed under Fe(II) polymerizing conditions.

Reduced U(IV) is present as nanoparticulate uraninite, coassociated with Fe in the solid phase, implying an inner sphere electron transfer mechanism.

M. I. Boyanov, E. J. O'Loughlin, E. E. Roden, J. B. Fein, K. M. Kemner, *Geochim. Cosmochim. Acta* **71** 1898-1912, 2007.

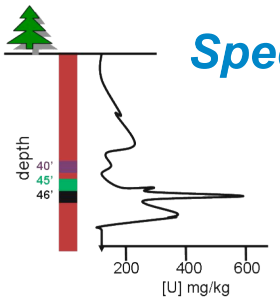

Speciation of Uranium in Sediments before and after in Situ Biostimulation

Shelly D. Kelly, Kenneth M. Kemner, Jack Carley, Craig Criddle, Phillip M. Jardine,
Terence L. Marsh, Debra Phillips, David Watson, Wei-Min Wu
acceptance pending minor revisions ES&T 2007

Before Biostimulation

Brown and Black region at 12.2 m and 14.0 m

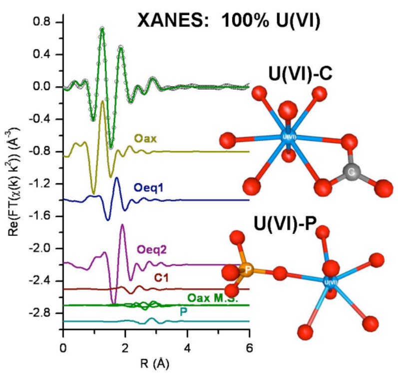

Greenish region at 13.7 m

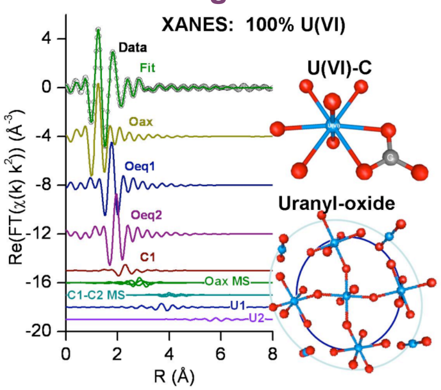

During Weekly Biostimulation Injections (monitoring wells) and After on Month of Cessation (injection well)

Monitoring Wells

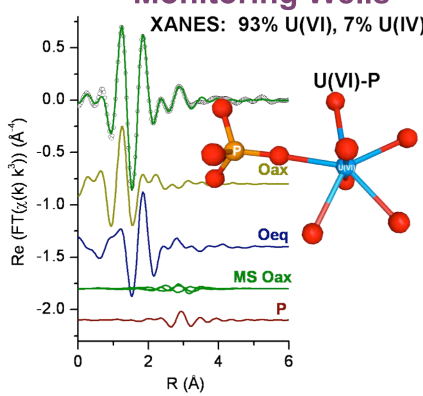

Injection Well

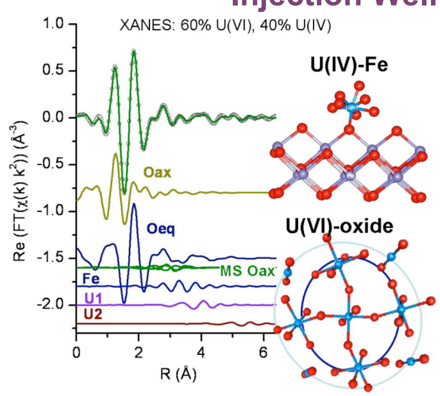

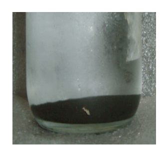

After One Year of Storage

Monitoring wells at 13.7 and 12.2 m

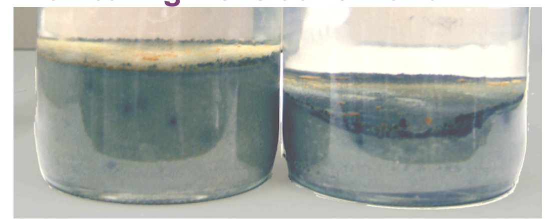

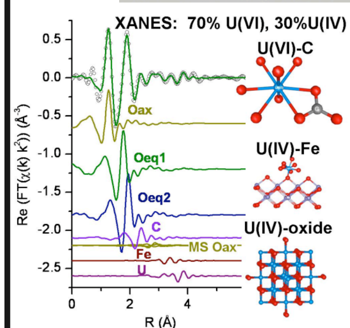

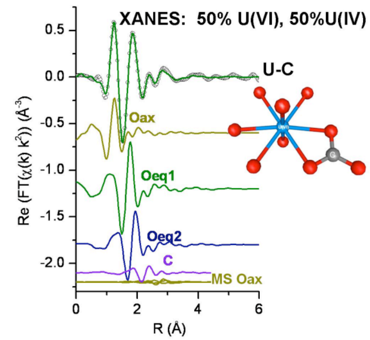

Injection well

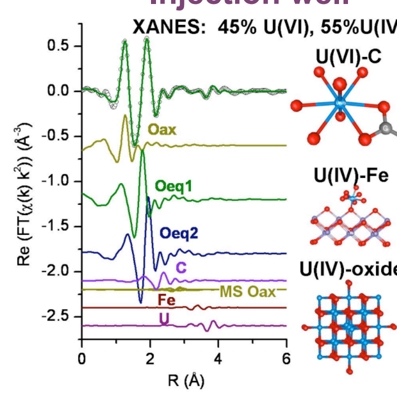

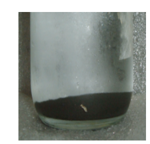

New ERSP Project: Monitoring U Transformation Determined by the Evolution of Biogeochemical Processes (S. D. Kelly, PI)

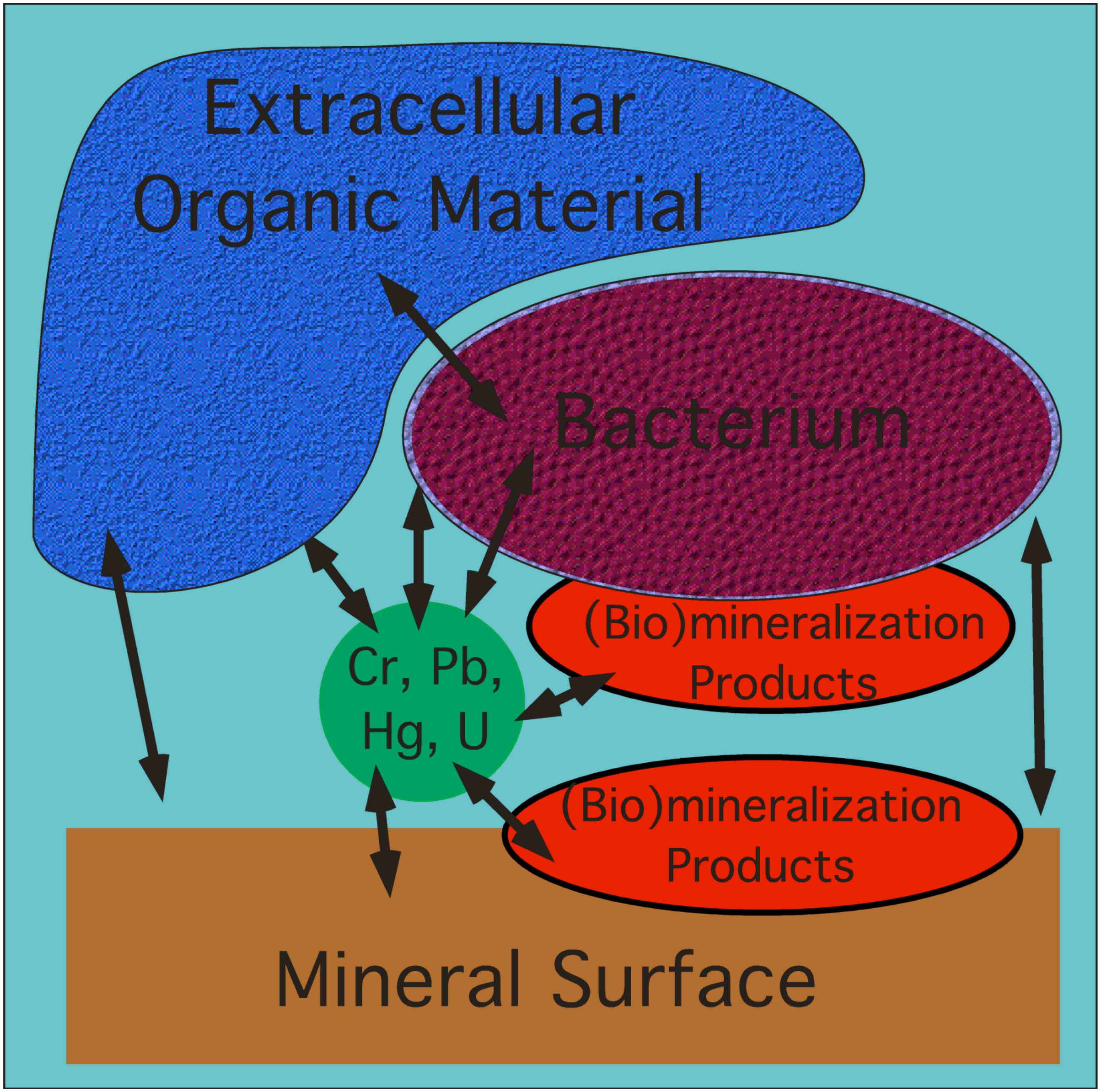

Kemner, O'Loughlin, Kelly, Boyanov, "Synchrotron x-ray investigations of mineral-microbe-metal interactions," ***Elements*** August 2005.

XRM with Fresnel zone plates:

X-RAY MICROPROBE BEAMLINE AT APS (2-ID-D/E)

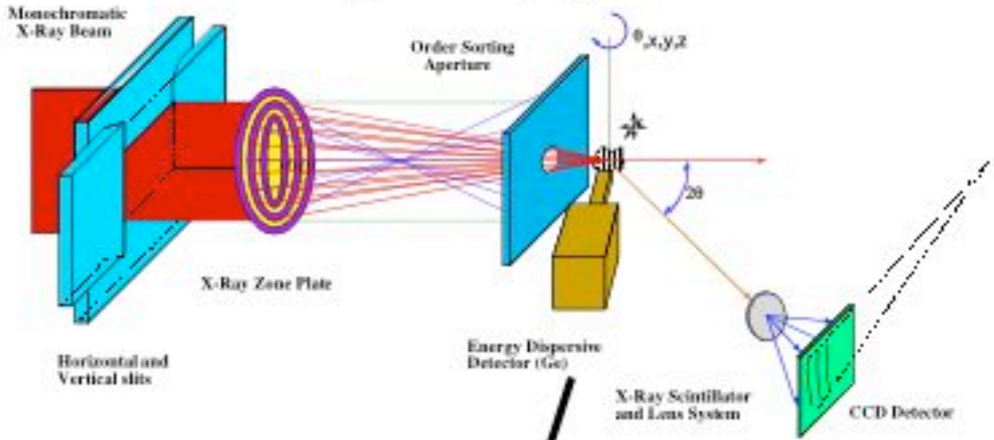

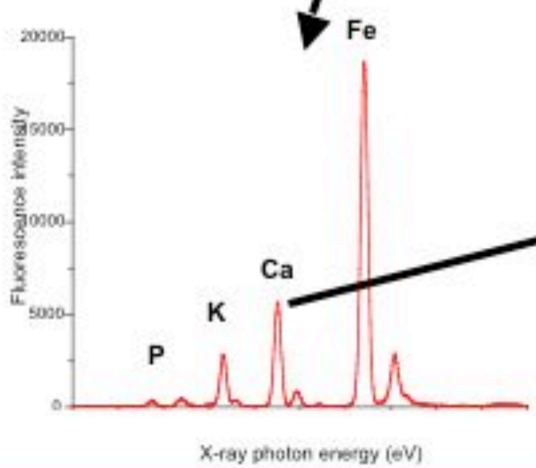

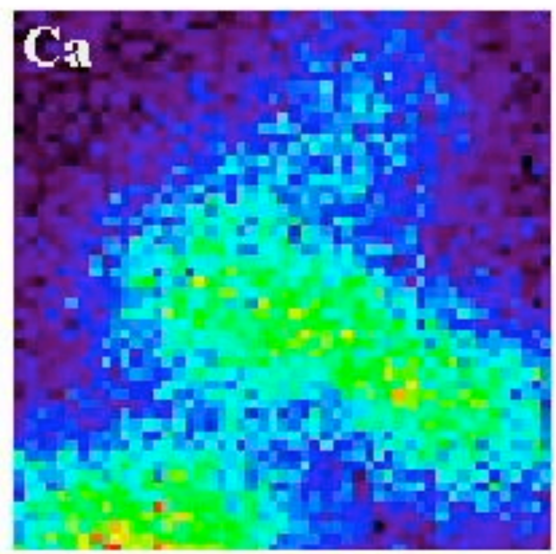

Resolution is dependent on the size of the x-ray probe - (~100nm).

Spatially resolve information provided by x-rays - (elements, chemical speciation).

9

Argonne NATIONAL LABORATORY

K. M. Kemner, et al., Science 306 686-687, 2004.

Biological Abundance

Major

Trace

1 H 1.01																	2 He 4.00
3 Li 6.94	4 Be 9.01											5 B 10.81	6 C 12.01	7 N 14.01	8 O 16.00	9 F 19.00	10 Ne 20.18
11 Na 22.99	12 Mg 24.31											13 Al 26.98	14 Si 28.09	15 P 30.97	16 S 32.06	17 Cl 35.45	18 Ar 39.95
19 K 39.10	20 Ca 40.08	21 Sc 44.96	22 Ti 47.88	23 V 50.94	24 Cr 52.00	25 Mn 54.94	26 Fe 55.85	27 Co 58.93	28 Ni 58.69	29 Cu 63.55	30 Zn 65.39	31 Ga 69.72	32 Ge 72.59	33 As 74.92	34 Se 78.96	35 Br 79.90	36 Kr 83.80
37 Rb 85.47	38 Sr 87.62	39 Y 88.91	40 Zr 91.22	41 Nb 92.91	42 Mo 95.94	43 Tc (98)	44 Ru 101.07	45 Rh 102.91	46 Pd 106.42	47 Ag 107.87	48 Cd 112.41	49 In 114.82	50 Sn 118.71	51 Sb 121.75	52 Te 127.60	53 I 126.91	54 Xe 131.29
55 Cs 132.91	56 Ba 137.33	57 La 138.91	72 Hf 178.49	73 Ta 180.95	74 W 183.85	75 Re 186.21	76 Os 190.2	77 Ir 192.22	78 Pt 195.08	79 Au 196.97	80 Hg 200.59	81 Tl 204.38	82 Pb 207.2	83 Bi 208.98	84 Po (209)	85 At (210)	86 Rn (222)
87 Fr (223)	88 Ra 226.03	89 Ac 227.03	104 Rf (261)	105 Ha (262)	106 Sg (263)	107 Ns (262)	108 Hs (266)	109 Mt (266)	110 Uun (269)	111 Uuu (272)	112 Uub (277)						

58 Ce 140.12	59 Pr 140.91	60 Nd 144.24	61 Pm (145)	62 Sm 150.36	63 Eu 151.96	64 Gd 157.25	65 Tb 158.93	66 Dy 162.50	67 Ho 164.93	68 Er 167.26	69 Tm 168.93	70 Yb 173.04	71 Lu 174.97
90 Th 232.03	91 Pa 231.04	92 U 238.03	93 Np 237.05	94 Pu (244)	95 Am (243)	96 Cm (247)	97 Bk (247)	98 Cf (251)	99 Es (252)	100 Fm (257)	101 Md (258)	102 No (259)	103 Lr (260)

A

XRF microscopy investigation of the localization of extracellular metalloproteins

Genomic analysis of the DMRB *S. oneidensis* MR-1 revealed it possesses several *c*-type cytochromes that are localized to the outer membrane (OM) and hypothesized to be involved in the reduction of U(VI) to $UO_{2(s)}$ in the form of nanoparticles. A mutant *(-MtrC/-OmcA*) was constructed that was deficient in two OM decaheme c-type cytochromes (MtrC and OmcA).

We have performed XRF elemental analysis of *S. oneidensis* MR-1 and mutant cells, and extracellular $UO_{2(s)}$ precipitates to investigate the location of high concentrations of Fe, consistent with the presence of metalloproteins.

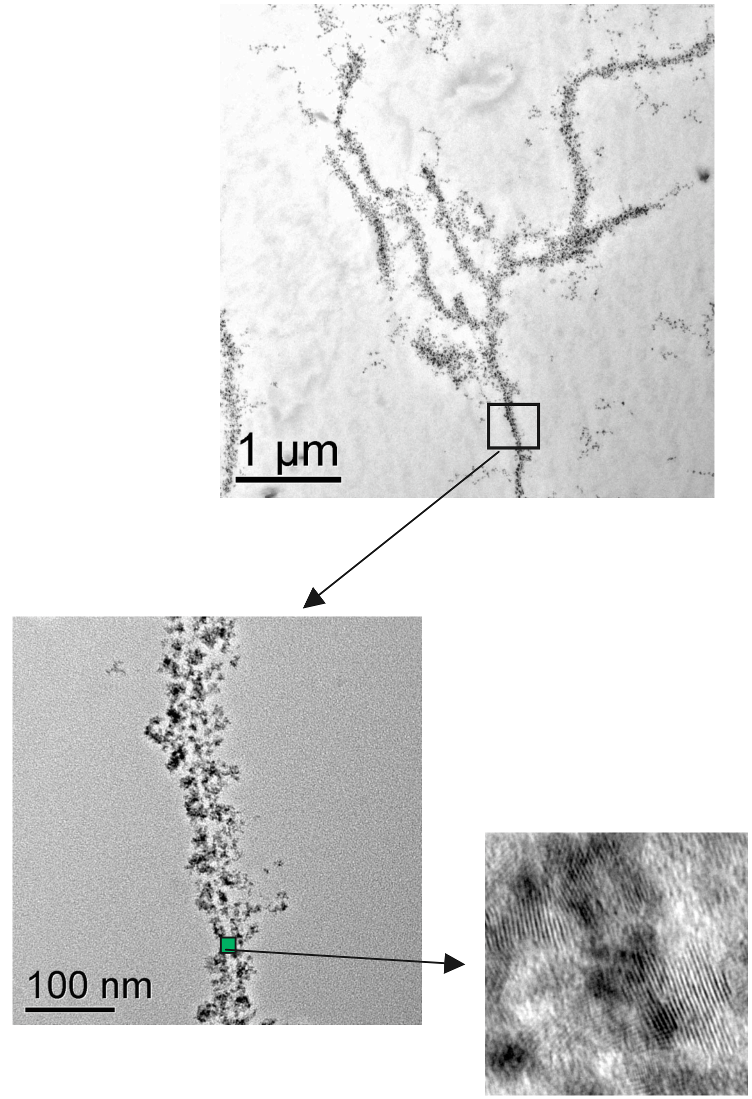

M. Boyanov, B. Lai, K. Kemner (ANL)
J. Fredrickson, J. Zachara, A. Beliaev, M. Marshall, A. Dohnalkova, D. Kennedy (PNNL)

XRF microscopy determination of co-localization of Fe, P, and U with cellular and extracellular material

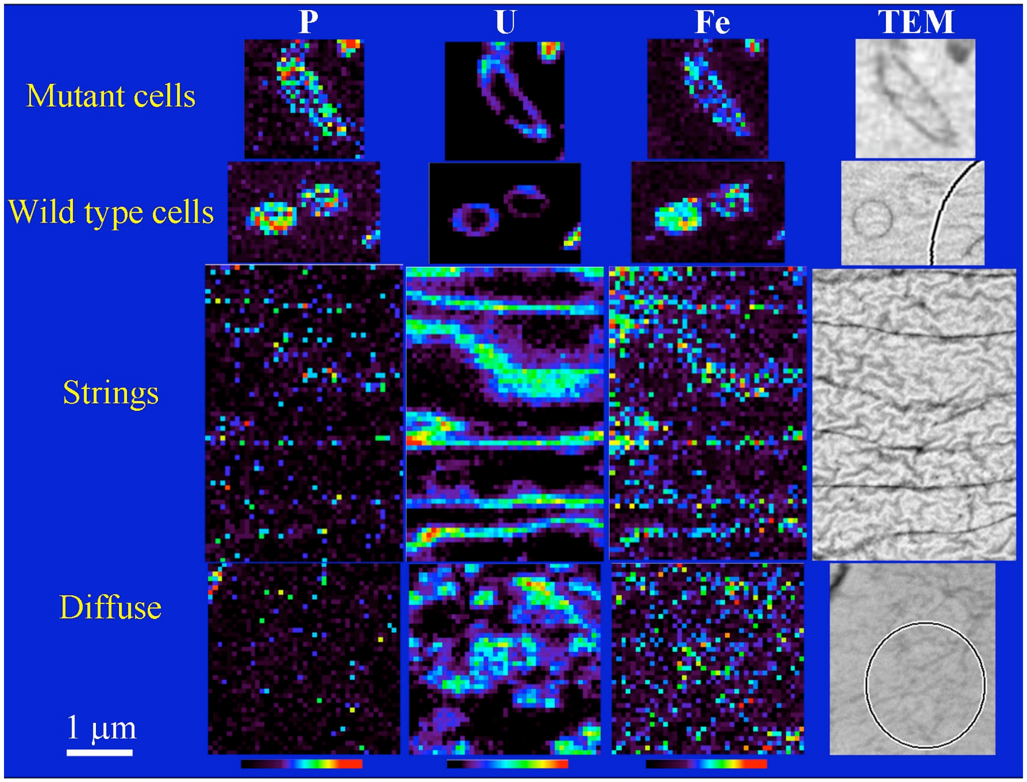

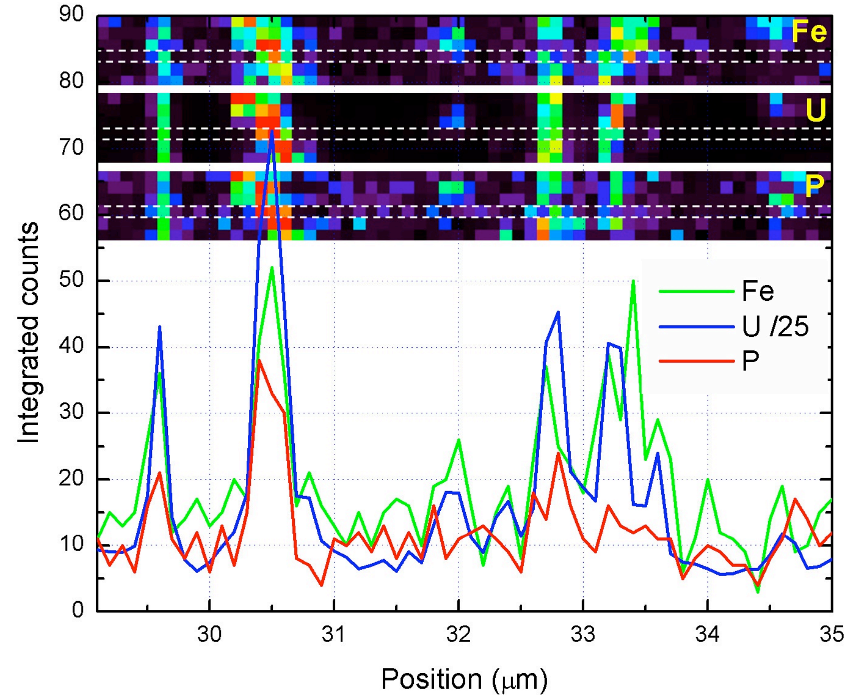

Cellular and extracellular co-localization of U, P, and Fe observed on fiber-like structures produced by *S. oneidensis* MR-1. Co-localization only peri-plasmic in mutant cells lacking the OM *c*-type cytochromes MtrC and OmcA.

Results are consistent with Fe-containing proteins associated with extra-cellular UO_2 fiber-like structures.

Bacterial resistance to radiation

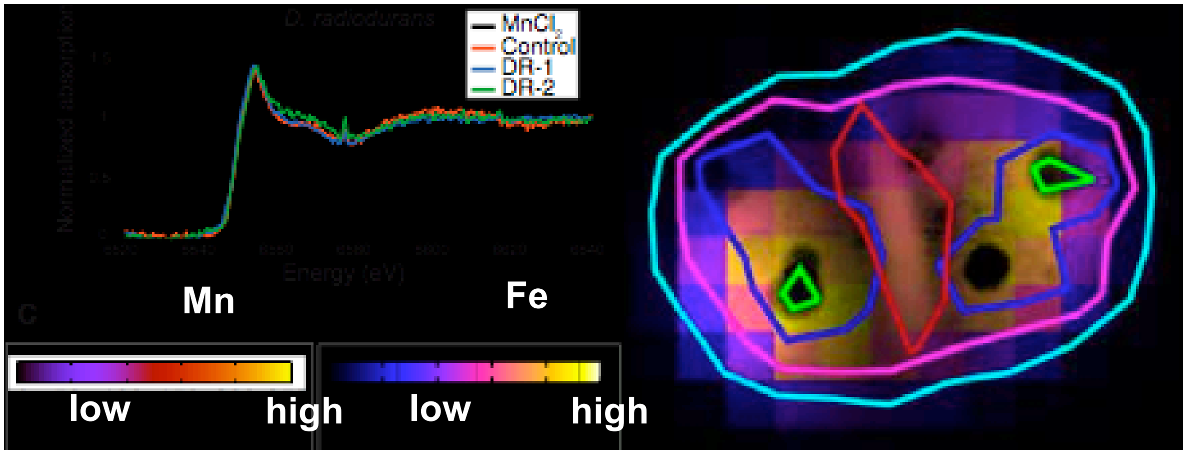

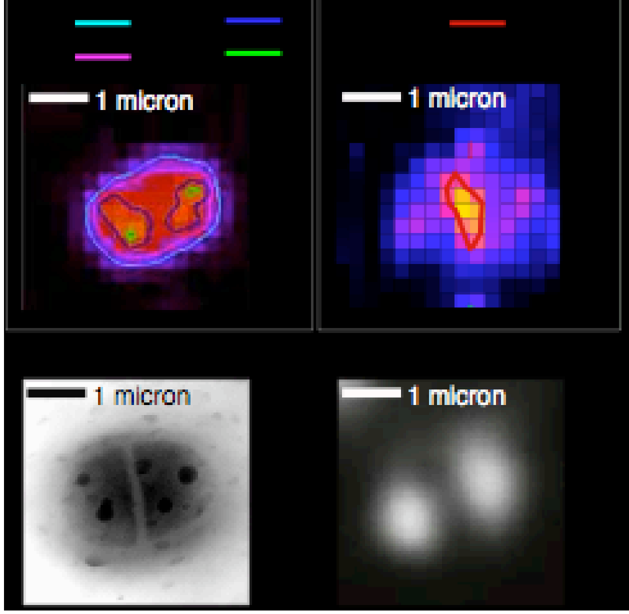

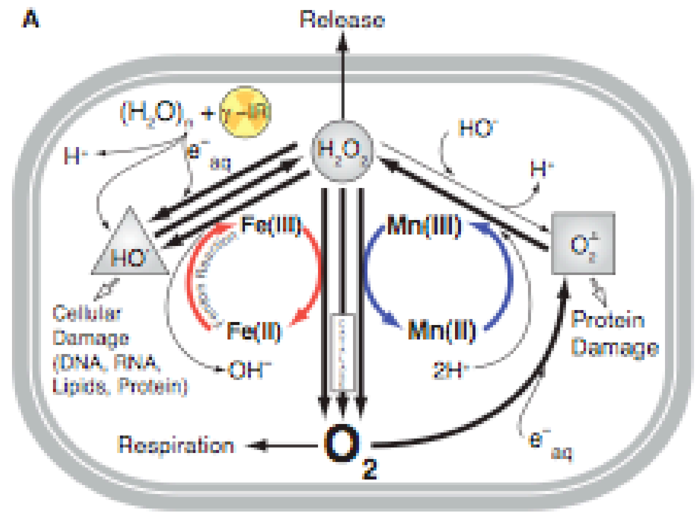

Radiation-induced cell death often attributed to DNA damage
Fe-facilitated Fenton reaction accentuates damage

High Mn/Fe ratios (*D. radiodurans*) resistant to radiation
Low Mn/Fe ratios (*S. oneidnesis*) less resistant to radiation
XRF microscopy shows
- -Mn ubiquitous throughout cell
- -Fe (Fenton reaction) between cells

Mn XAFS shows Mn2+ throughout cell
- -facilitates superoxide scavanging

Radiation damage caused by protein oxidation during irradiation

M. J. Daly, et al., "Protein Oxidation Implicated as the Primary Determinant of Bacterial Radioresistance," ***PLoS Biology*, Vol. 5, No.4**

Coupled Microbial, Geochemical, and Mineralogical Controls on Biogenic Fe(II) Speciation and Reactivity

Ed O'Loughlin, Ken Kemner, Carol Giometti, Shelly Kelly, & Bruce Ravel (ANL)
Michele Scherer (University of Iowa)
Maxim Boyanov (University of Sofia)
Michael McCormick (Hamilton College)
Robert Sanford (University of Illinois at Urbana-Champaign)

Biogeochemical controls on biogenic Fe(II) speciation

- Effects of microbial physiology (e^- donor utilization across broad range of Fe(III)-reducing bacteria)
- Solution chemistry effects (pH, $[CO_3]_{TOT}$, $[P0_4]_{TOT}$, etc.)
- Effects of Fe(III) mineralogy (Fe(III) oxides/oxyhydroxides, Fe(III)-bearing clay minerals, and natural mineral assemblages)

Differential redox reactivity of biogenic Fe(II) species

- Systematic investigation of the effects of biogenic Fe(II) speciation on contaminant reduction

"Abiotic" vs Microbial vs Microbially Mediated Contaminant Reduction

"Abiotic"

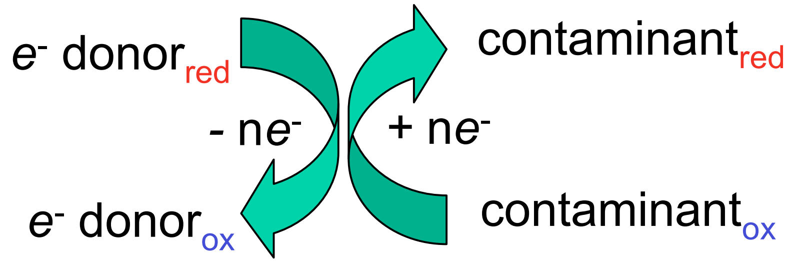

Microbial

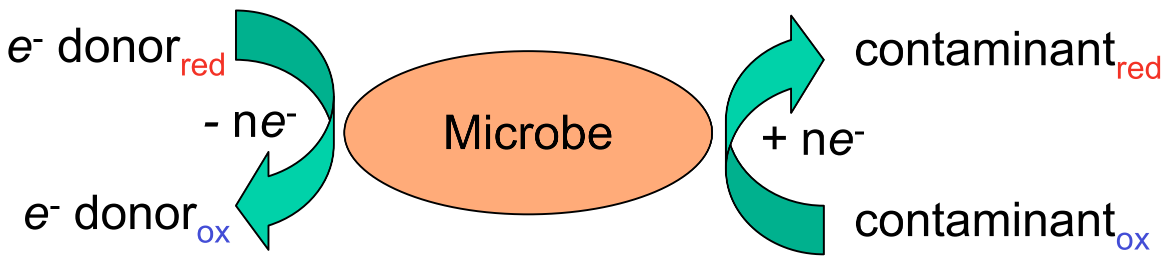

Microbially Mediated

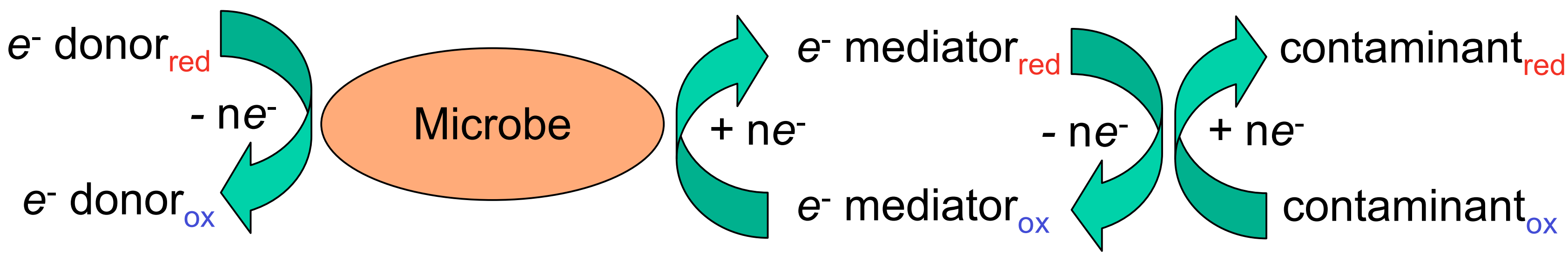

Microbial Fe(III) Reduction

Organic C_{red}
H_2

- ne⁻

Organic C_{ox}
H^+
CO_2

Soluble Fe^{III}

Ferrihydrite

Hematite

Goethite

Lepidocrocite

Structural Fe^{III} In Clays

Fe^{III}

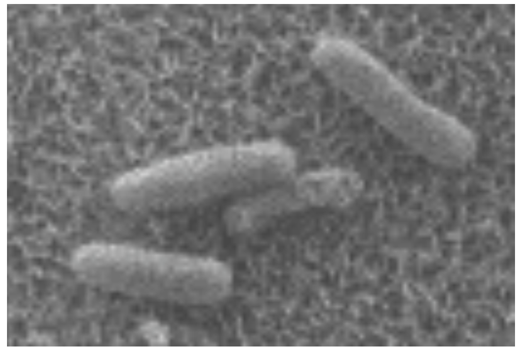

Shewanella oneidensis MR-1

Fe^{II}

✓ Soluble Fe^{II}

✓ Sorbed Fe^{II}

✓ Magnetite

✓ Green Rust

Siderite

Vivianite

✓ Structural Fe^{II} In Clays

✓ Effective reductants for many organic and inorganic contaminants

Green Rusts have been shown to reduce U(VI)[1], Cr(VI), Tc(VII), Hg(II)[2], nitrate, some chlorinated solvents, nitroaromatics, Se(VII) & others

(1) O'Loughlin, E.J., S.D. Kelly, R.E. Cook, R. Csencsits and K.M. Kemner. 2003. ***Reduction of uranium(VI) by mixed Fe(II)/Fe(III) hydroxide (green rust): Formation of UO_2 nanoparticles***. ES&T. 37: 721-727.

(2) O'Loughlin, E.J., S.D. Kelly, K.M. Kemner, R. Cesncsits, and R.E. Cook. 2003. ***Reduction of Ag(I), Au(III), Cu(II), and Hg(II) by Fe(II)/Fe(III) hydroxysulfate green rust***. Chemosphere 53: 437-446.

Differential Redox Reactivity of Biogenic Fe(II) Species

Formation of Biogenic Fe(II) Phases

Experimental System

160-mL serum vial
100 mL Minimal Medium
75 mM *e*$^-$ donor
80 mM Fe(III)
~5 ×10^9 cells mL$^{-1$}
typically *S. putrefaciens CN32*

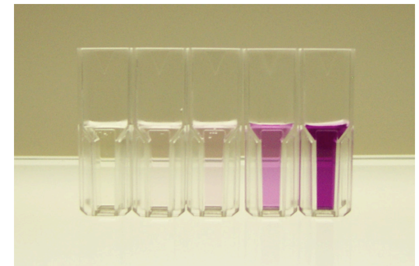

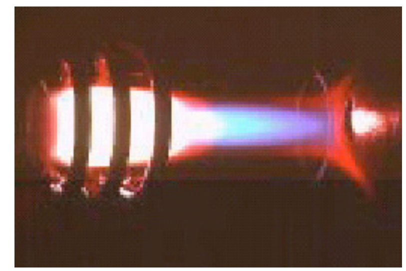

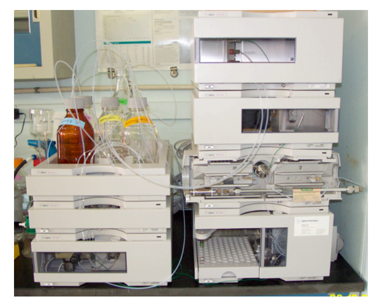

pH

Fe(II)

Total Fe/Fe(III)

[e$^-$ donor]

Solids

O'Loughlin, E. J., P. Larese-Casanova, R. E. Cook, and M. M. Scherer. (In press). ***Green rust formation from dissimilatory iron reduction of γ-FeOOH (lepidocrocite): Comparison of several Shewanella species***. Geomicrobiol. J.

Formation of Biogenic Fe(II) Phases

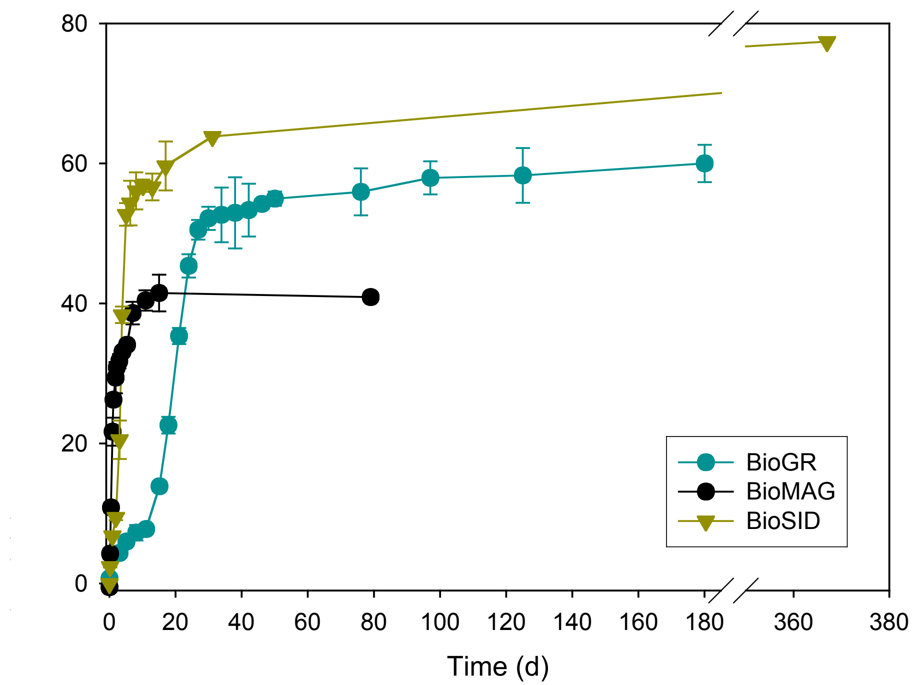

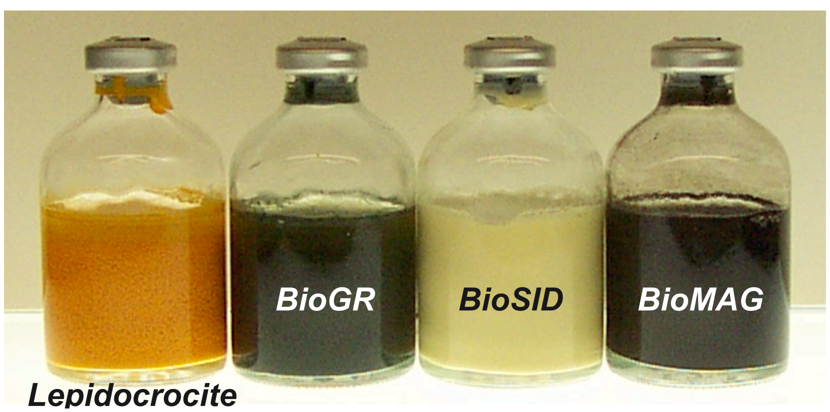

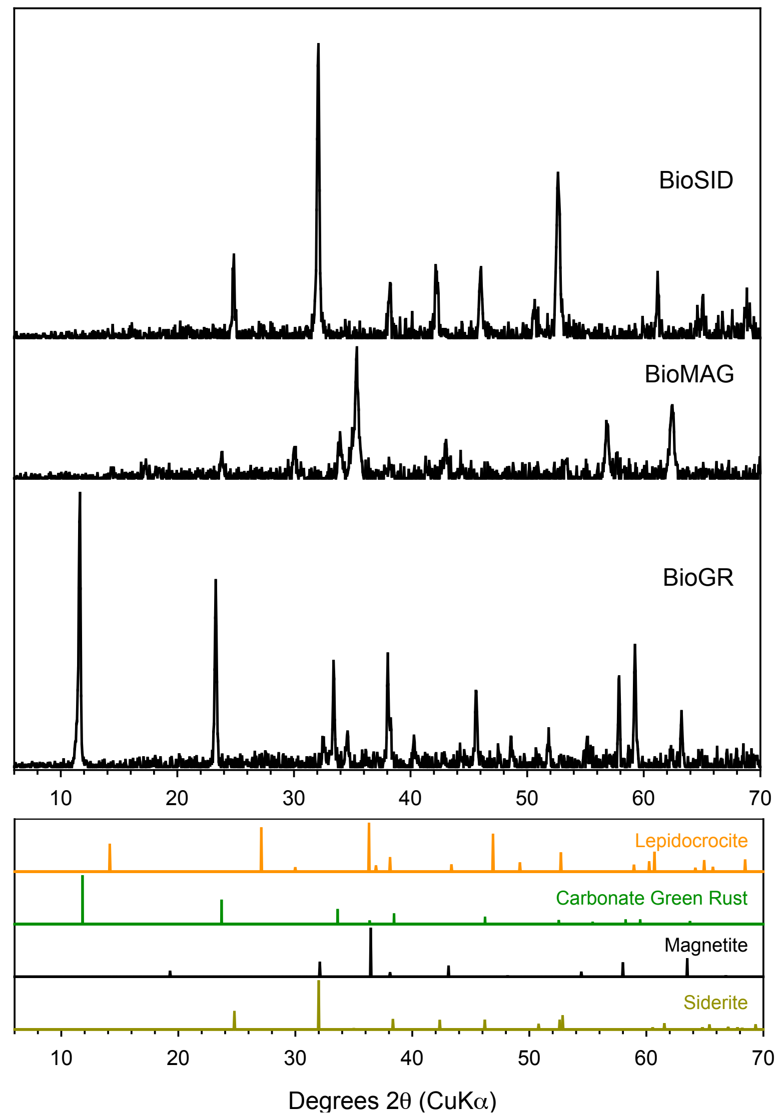

O'Loughlin, E.J., P. C.A. Gorski, R.E. Cook, and M.M. Scherer. (in preparation). ***Electron donor effects on the bioreduction of lepidocrocite by Shewanella putrefaciens CN32***. Geomicrobiol. J

U(VI) Interaction with Biogenic Fe(II) Phases

Experimental System

pH

U speciation

U XAFS

Total U

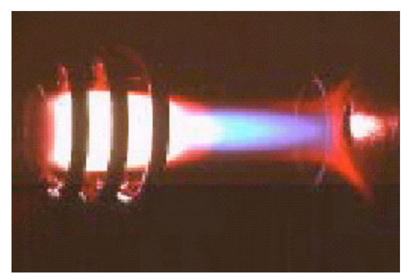

Biogenic Fe(II) phase
Pasteurized 70 ˚C
Washed/sonicated
~60 mM Fe(II)

Add 500 μM U(VI)

Within 48 h > 98% of added U associated with solids

Sorption or Reduction??????

O'Loughlin, E.J., S.D. Kelly, and K.M Kemner. (in preparation). ***Reduction of U(VI) by products of the bioreduction of Fe(III) oxides***. Environ. Sci. Technol.

U L_{III}–edge EXAFS Results for U(VI) Interaction with Biogenic Green Rust

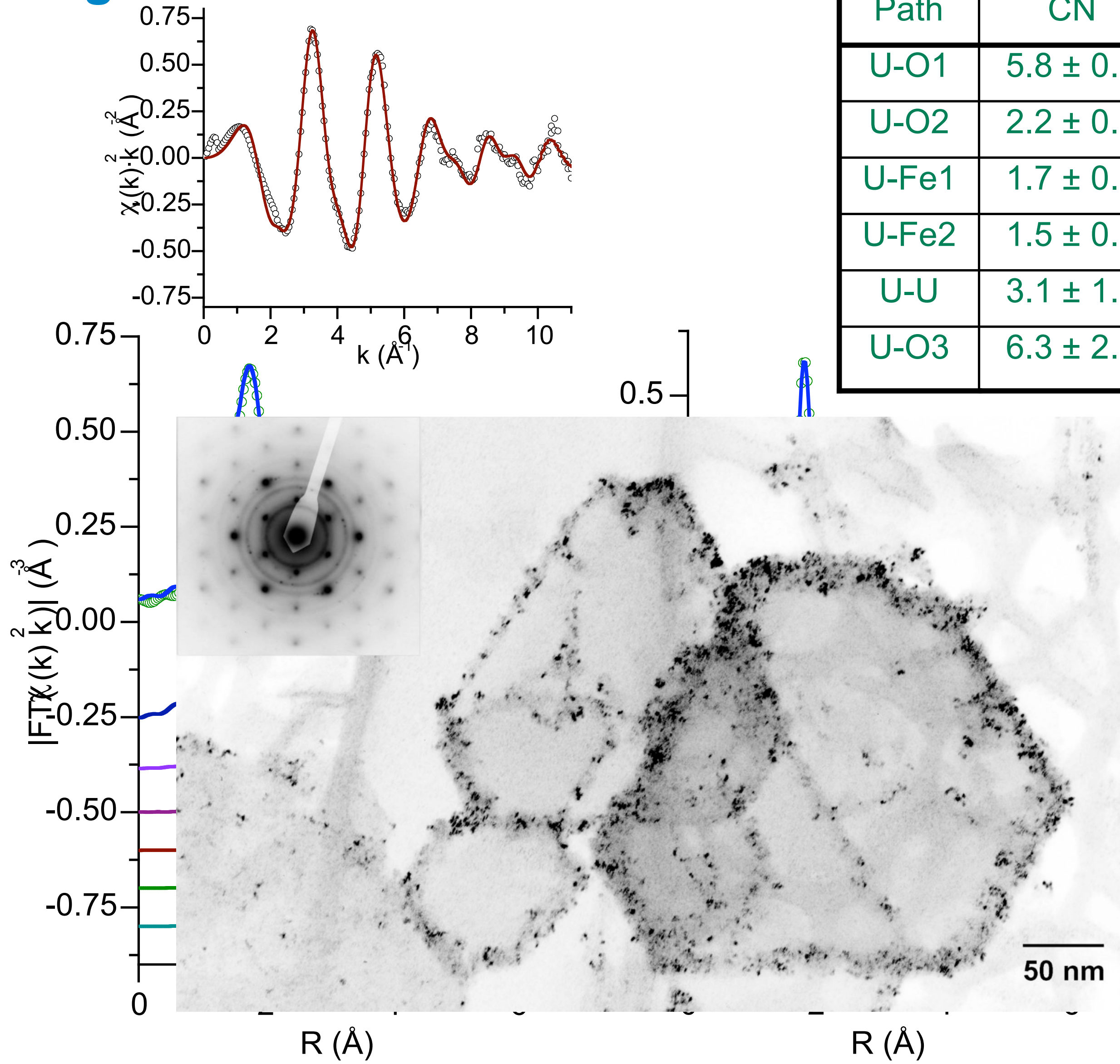

Path	CN	R (Å)	sigma² (x10⁻³ Å²)
U-O1	5.8 ± 0.5	2.33 ± 0.01	9.5 ± 1.7
U-O2	2.2 ± 0.5	2.57 ± 0.04	9.5 ± 1.7
U-Fe1	1.7 ± 0.9	2.86 ± 0.02	13.6 ± 4.2
U-Fe2	1.5 ± 0.8	3.47 ± 0.03	13.6 ± 4.2
U-U	3.1 ± 1.0	3.80 ± 0.03	13.6 ± 4.2
U-O3	6.3 ± 2.0	4.81 ± 0.14	27.2 ± 8.4

Uraninite

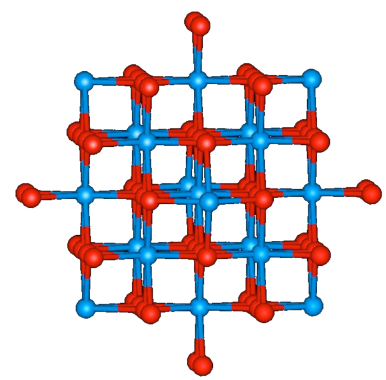

8 O at 2.35 Å

12 U at 3.87 Å

0 ± 10% U(VI)

U L_{III}-edge EXAFS Results for U(VI) Interaction with Biogenic Magnetite

Path	CN	R (Å)	sigma^2 (x10^{-3} Å^2)
U-Oax	0.8 ± 0.2	1.75 ± 0.02	11.2 ± 6.6
U-O2	7.2 ± 0.4	2.38 ± 0.01	16.3 ± 1.1
U-Fe1	0.5 ± 0.4	2.86 ± 0.05	12.0 ± 4.0
U-Fe2	1.4 ± 0.7	3.46 ± 0.03	12.0 ± 4.0
U-U	3.4 ± 1.4	3.86 ± 0.03	12.0 ± 4.0
U-O2	6.7 ± 2.8	5.01 ± 0.20	24.0 ± 7.9

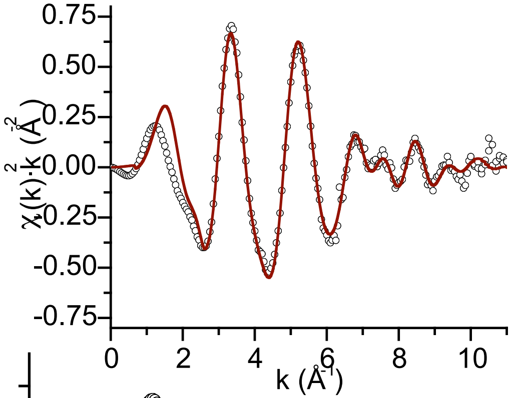

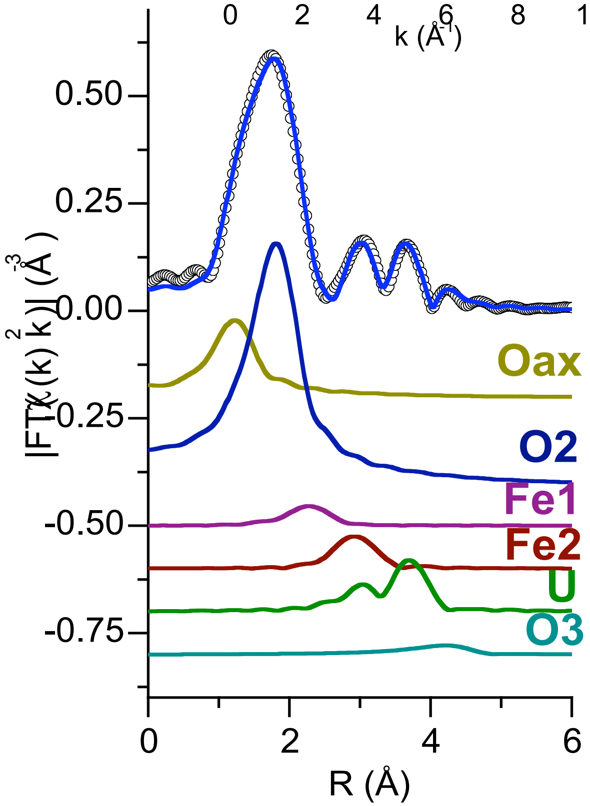

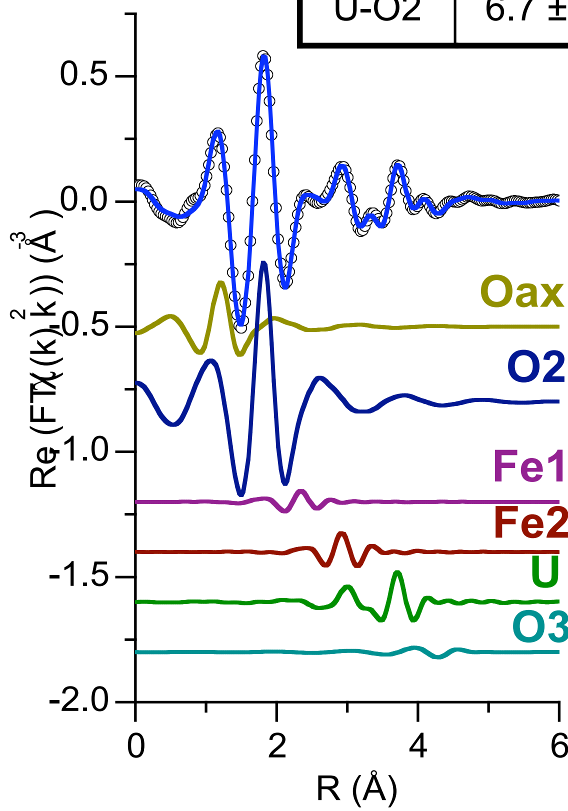

40 ± 10% U(VI)

U L_{III}-edge EXAFS Results for U(VI) Interaction with Biogenic Siderite

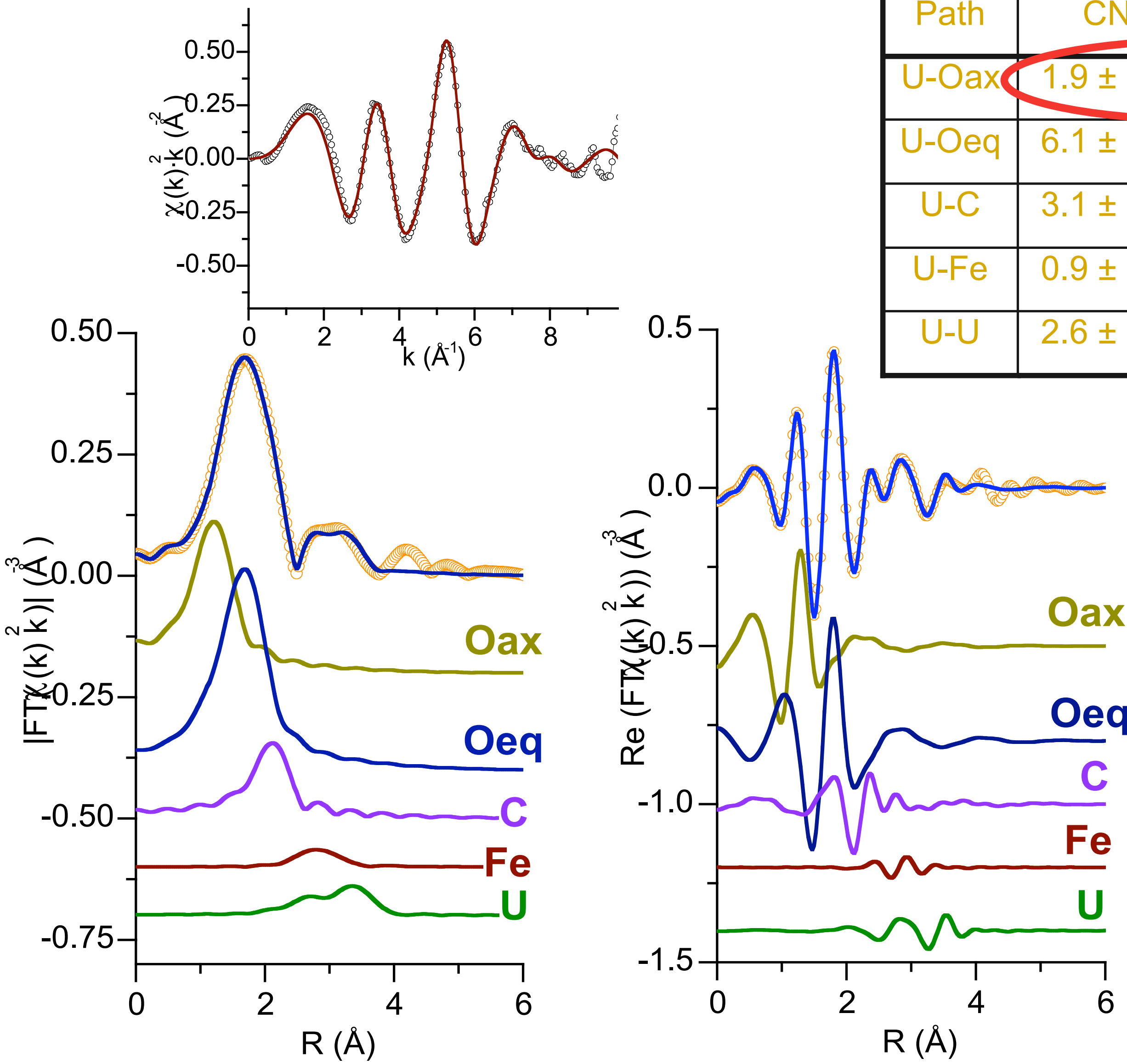

Path	CN	R (Å)	sigma² (x10⁻³ Å²)
U-Oax	1.9 ± 0.7	1.80 ± 0.01	13.4 ± 5.5
U-Oeq	6.1 ± 0.7	2.31 ± 0.03	19.3 ± 3.3
U-C	3.1 ± 0.7	2.86 ± 0.01	5.0
U-Fe	0.9 ± 0.5	3.43 ± 0.04	14.0
U-U	2.6 ± 0.6	3.63 ± 0.05	18.4

95 ± 20% U(VI)

Differential Redox Reactivity of Biogenic Fe(II) Phases

Differential redox reactivity of biogenic Fe(II) species

- Rapid and complete reduction of U(VI) by biogenic green rust
- Partial reduction of U(VI) by biogenic magnetite (kinetics?)
- Siderite an effective sorbent for U(VI) (stability), but no reduction

Future studies will focus on

- Solution chemistry effects; parameters affecting U(VI) speciation in particular (pH, $[CO_3]_{TOT}$, cations, organic ligands, etc.)
- Quantitative determination of uptake/reduction kinetics
- Stability of reduced/sequesterd U

Summary

- **An improved understanding of fundamental coupled biogeochemical processes obviously is critical for decision making for environmental remediation and long-term stewardship.**

- **Synchrotron x-ray radiation provides the most versatile and powerful approach for directly determining the chemical speciation of the radionuclide and heavy metal contaminants of concern to DOE.**

- **Integration of synchrotron approaches with integrated multidisciplinary scientific investigations provides a powerful way of understanding coupled biogeochemical processes whereby the scientific question drives the development of new synchrotron-based technologies and the unique information provided by the synchrotron-based technology enables the development of new scientific hypotheses and insights.**